



## RESEARCH LETTER

10.1002/2014GL059519

## Key Points:

- JRA-55 appears to be the best reanalysis reproducing observed TC climatology
- The finest resolution reanalysis are not always the best in TC climatology
- Most of the reanalysis data sets show reasonable TC distribution globally

## Supporting Information:

- Readme
- Figure S1
- Figure S2
- Figure S3
- Table S1
- Text S1

## Correspondence to:

H. Murakami,  
hir.murakami@gmail.com

## Citation:

Murakami, H. (2014), Tropical cyclones in reanalysis data sets, *Geophys. Res. Lett.*, 41, 2133–2141, doi:10.1002/2014GL059519.

Received 4 FEB 2014

Accepted 28 FEB 2014

Accepted article online 3 MAR 2014

Published online 24 MAR 2014

## Tropical cyclones in reanalysis data sets

Hiroyuki Murakami<sup>1</sup><sup>1</sup>International Pacific Research Center, University of Hawai'i at Mānoa, Honolulu, Hawaii, USA

**Abstract** This study evaluates and compares tropical cyclones (TCs) in state-of-the-art reanalysis data sets including the following: the Japanese 55-year Reanalysis (JRA-55), Japanese 25-year Reanalysis, European Centre for Medium-Range Weather Forecasts Reanalysis-40, Interim Reanalysis, National Centers for Environmental Prediction Climate Forecast System Reanalysis, and NASA's Modern Era Retrospective Analysis for Research and Application (MERRA). Most of the reanalyses reproduce a reasonable global spatial distribution of observed TCs and temporal interannual variation of total TC frequency. Of the six reanalysis data sets, JRA-55 appears to be the best in terms of the following: the highest skill for spatial and temporal distribution of TC frequency of occurrence, highest TC hitting rate, lower false alarm rate, reasonable TC structure in terms of the relationship between maximum surface wind speed and sea level pressure, and higher correlation coefficients for interannual variations of TC frequency. These results also suggest that the finest-resolution reanalysis data sets, like MERRA, are not always the best in terms of TC climatology.

## 1. Introduction

Global reanalyses have been conducted at major numerical weather prediction centers around the world. Over the last decade, the most widely used reanalysis data sets are as follows: the European Centre for Medium-Range Weather Forecasts (ECMWF) Reanalysis-40 (ERA-40) [Uppala *et al.*, 2005] and Interim Reanalysis (ERA-Interim) [Dee *et al.*, 2011]; the National Centers for Environmental Prediction (NCEP)/National Center for Atmospheric Research (NCAR) Reanalysis 1 (NCEP-1) [Kalnay *et al.*, 1996; Kistler *et al.*, 2001] and Reanalysis 2 (NCEP-2) [Kanamitsu *et al.*, 2002]; and the Japanese 25-year Reanalysis (JRA-25) [Onogi *et al.*, 2007] by Japan Meteorological Agency (JMA) and Central Research Institute of Electric Power Industry. These reanalyses provided researchers with fundamental climate states and variability that are dynamically consistent by utilizing unchanged frameworks of data assimilation schemes and models over the analysis period.

Tropical cyclones (TCs) (or TC-like vortices) in reanalysis data sets are commonly used as a reference for observations when evaluating simulated TCs by general circulation models [Murakami and Sugi, 2010; Bell *et al.*, 2013; Strachan *et al.*, 2013; Rathmann *et al.*, 2014]. These data are also used to study climate variability. Scoccimarro *et al.* [2012] indicated that a good representation of TCs in a reanalysis is important in the study of the interaction between TCs and the climate system.

Reanalyses have been also used as lateral boundary conditions for regional climate models. One example is the future warming projection, the so-called pseudo global warming method [Kimura and Kitoh, 2007], in which initial and boundary conditions for the regional model integrations are given by a reanalysis and a perturbation or global warming increment is estimated from simulations with global coupled models [e.g., Knutson *et al.*, 2008; Kawase *et al.*, 2009; Lauer *et al.*, 2013]. Therefore, it is important that the reanalysis includes accurate climate mean states as well as accurate information on structure, location, and distribution of small-scale disturbances such as TCs at a time scale of 6-hourly or daily for addressing the possible impact of global warming on TCs. However, the typical horizontal resolution of the output of the reanalysis data sets is between  $2.5^\circ \times 2.5^\circ$  and  $1.25^\circ \times 1.25^\circ$ , which is too low to resolve observed TC inner structure. Therefore, current regional climate modeling studies mainly forced with large-scale data (e.g., wave numbers 0–2) from the reanalysis data set (i.e., the so-called spectral nudging) [Waldron *et al.*, 1996] and generated other high-frequency fields using the model itself.

Recently, high-resolution reanalyses have become available to researchers. Examples of these include the NCEP Climate Forecast System (CFRS;  $0.5^\circ \times 0.5^\circ$ ) [Saha *et al.*, 2010] by NOAA and the Modern Era Retrospective Analysis for Research and Applications (MERRA;  $0.6^\circ \times 0.5^\circ$ ) [Rienecker *et al.*, 2011] by NASA.

**Table 1a.** List of Reanalysis Data Sets and Their Configuration

Name	Reference	Analysis Period	Resolution for Assimilation	Resolution for Output
Japanese 25-year Reanalysis	<i>Onogi et al.</i> [2007]	1979–2012	$T_{106}$ (120 km)	$1.25^\circ \times 1.25^\circ$ (140 km)
Japanese 55-year Reanalysis	<i>Ebita et al.</i> [2011]	1958–2012	$T_L 319$ (60 km)	$1.25^\circ \times 1.25^\circ$ (140 km)
ECMWF Reanalysis-40	<i>Uppala et al.</i> [2005]	1958–2001	$T_L 159$ (120 km)	$2.5^\circ \times 2.5^\circ$ (280 km)
ECMWF Interim Reanalysis	<i>Dee et al.</i> [2011]	1979–2012	$T_L 255$ (80 km)	$1.5^\circ \times 1.5^\circ$ (170 km)
NCEP Climate Forecast System Reanalysis	<i>Saha et al.</i> [2010]	1979–2012	$T_{382}$ (40 km)	$0.5^\circ \times 0.5^\circ$ (60 km)
NASA's Modern Era Restrospective analysis for Research and Applications	<i>Rienecker et al.</i> [2011]	1979–2012	(60 km)	$0.6^\circ \times 0.5^\circ$ (60 km)

Another development is the new Japanese 55-year Reanalysis (JRA-55;  $1.25^\circ \times 1.25^\circ$ ) [Ebita et al., 2011], which is about to open to the public. It is expected that JRA-55 will give a more accurate reanalysis of TC climatology with higher resolution than JRA-25 in its data assimilation system. Although Strachan et al. [2013] analyzed TCs in ERA-40, ERA-Interim, and MERRA using their unique TC detection method, it is not clear which reanalysis is the best in terms of climatological and temporal variation of TCs because their main goal was to compare TCs simulated by general circulation models.

In this study, we evaluate TCs from state-of-the-art reanalysis data sets using 6-hourly data. This study aimed to address which of the reanalysis is the best in terms of spatial and temporal variation of TCs as well as intensity and structure. Section 2 provides a description of the reanalysis data sets, observed data sets, and TC detection methods. Section 3 presents the results. Finally, a summary is given in section 4.

## 2. Methods

### 2.1. Reanalysis Data Sets

The reanalysis data sets used in this study are summarized in Tables 1a–1f. They are the state-of-the-art reanalyses released after 2004. The reanalysis with the highest horizontal resolution for output is CFSR ( $0.5^\circ \times 0.5^\circ$ ), followed by MERRA ( $0.6^\circ \times 0.5^\circ$ ), and JRA-55 and JRA-25 ( $1.25^\circ \times 1.25^\circ$ ). All the reanalysis data sets are overlapped in their analysis period 1979–2012 except for ERA-40 (up to 2001); therefore, all intercomparisons in this study are made for the common period of 1979–2012 (1979–2001 for ERA-40). In addition, JRA-55 and ERA-40 cover the long-term period from 1958. We compare the interannual variation of TCs in these reanalyses from the period 1958–2012 (1958–2001 for ERA-40) over the basins of the western North Pacific (WNP), eastern North Pacific (ENP), and North Atlantic (NAT). The observations from these basins are considered more reliable than those for the other ocean basins for the long-term period. The analyses considered total global (GL) results and results for six ocean basins: North Indian Ocean (NIO), WNP, ENP, NAT, South Indian Ocean (SIO), and South Pacific Ocean (SPO) (see Figure 1 for regional boundaries).

### 2.2. Observational Data Sets

The observed TC “best-track” data were obtained from the International Best Track Archive for Climate Stewardship (IBTrACS v03r05) [Knapp et al., 2010] and used to evaluate the TCs in the reanalyses. Because IBTrACS v03r05 provides information on a specific storm from different regional observational centers, we can choose our preferred data source. Here we use two collections of the global data set from the IBTrACS v03r05: the World Meteorological Organization (WMO)-sanctioned forecast agencies (IBTrACS\_wmo) and the collection from the National Hurricane Center (NHC) and Joint Typhoon Warning Center (JTWC) (IBTrACS\_nhcjtwc). Because WMO agencies apply different time lengths for averaging surface wind speed (e.g., WMO New Delhi (Tokyo) applies 3 min (10 min) for averaging sustained maximum wind speed), we converted the maximum wind speed to the equivalent 1 min sustained surface wind speed by using a factor of 1.0302 (1.1359) for a 3 min (10 min) wind speed. These factors originate from Simiu and Scanlon [1978] who noted that the strength of a

**Table 1b.** Applied TC Detection Criteria by Murakami and Sugi [2010]

	JRA-25	JRA-55	ERA-40	ERA-Interim	CFSR	MERRA
$\zeta_{850} (\times 10^{-5} s^{-1})$	1.0	1.0	1.0	8.1	15.0	1.0
$t_a$ (K)	0.6	0.9	0.8	1.0	1.3	1.0
$d$ (h)	36	36	24	24	36	30

**Table 1c.** Detected Annual Mean TC Number for Each TC Detection Method (1979–2012, Observed = 83.4–84.3)

	JRA-25	JRA-55	ERA-40	ERA-Interim	CFSR	MERRA
<i>Murakami and Sugi</i> [2010]	83.7	83.9	83.7	83.8	83.9	83.6
<i>Walsh et al.</i> [2007]	33.2	39.6	47.6	34.5	86.0	9.9
<i>Strachan et al.</i> [2013]	82.7	92.3	69.1	68.0	87.2	39.3

10 min sustained wind speed is statistically 88% of the 1 min sustained wind speed. We only used TCs with tropical storm intensities or stronger (i.e., TCs possessing 1 min sustained surface winds of 35 kt or greater) during the period 1958–2012. We also removed TC tracks that reportedly transformed to extratropical cyclones. Note that IBTrACS\_wmo does not contain any TCs before 1990 in the NIO.

### 2.3. TC Detection Methods

So far, a number of TC detection methods for reanalyses and model outputs have been proposed [*Walsh et al.*, 2007]. It is possible that the evaluation results depend on the TC detection method used. Here we applied a TC detection method by *Murakami and Sugi* [2010] as well as two additional methods proposed by *Walsh et al.* [2007] and *Strachan et al.* [2013] in order to test the influence of different TC detection methods on the results. A more detailed description of the TC detection methods is given in the supporting information. These TC detection methods are generally similar in terms of using surface maximum wind speed or low-level vorticity ( $\zeta_{850}$ ), temperature anomaly ( $t_a$ ), and duration ( $d$ ) as criteria; however, there are critical differences among them. In the detection method by *Murakami and Sugi* [2010], the criteria are optimized for each reanalysis so that the detected annual mean TC number becomes an observed number of about 83–84. This method assumes that TC intensity in a low-resolution reanalysis should be underestimated compared to observations; therefore, the TC detection criteria should be relaxed. Table 1b shows reanalysis-dependent criteria used in this study.

The TC detection by *Walsh et al.* [2007], which was originally developed by *Walsh et al.* [2004], assumes that the observed profile of TC intensity is dependent on horizontal resolution. The observed definition of TC genesis is 34kt ( $17.5 \text{ m s}^{-1}$ ), the observed azimuthal mean TC intensity profile is interpolated to a certain resolution, and the interpolated maximum wind speed is used for TC detection criteria for the resolution [see Figure 2 of *Walsh et al.*, 2007]. In this study, we applied the resolution-dependent criterion of maximum wind speed for each reanalysis as follows:  $14 \text{ m s}^{-1}$  for JRA-25 and JRA-55;  $11 \text{ m s}^{-1}$  for ERA-40;  $13.5 \text{ m s}^{-1}$  for ERA-Interim; and  $16.5 \text{ m s}^{-1}$  for CFSR and MERRA.

*Strachan et al.* [2013] is another TC detection method used in this study. In this method, the vorticity field in the original resolution is converted to T42 resolution and TC candidates are searched using a fixed vorticity criterion of  $0.5 \times 10^{-5} \text{ s}^{-1}$ . For the second step, the vorticity field in the original resolution is converted to T63 resolution and the final TC candidates are searched using a fixed criterion of  $6.0 \times 10^{-5} \text{ s}^{-1}$ . In addition to these vorticity criteria, there are additional constraints: low-level maximum vorticity should be larger than upper levels, and these conditions should last at least 1 day. This method does not require any resolution or reanalysis-dependent criteria. Moreover, only wind fields are required for TC detection.

## 3. Results

### 3.1. Number of TCs

Table 1c compares the annual mean of the detected TC number for each reanalysis data set using different TC detection methods. Using *Murakami and Sugi* [2010], the mean detected number is, in fact, about 84 because the TC number is optimized by reanalysis-dependent TC detection criteria. TCs detected using *Walsh et al.* [2007]

**Table 1d.** Scores for the Global TC Frequency of Occurrence Detected Using *Murakami and Sugi* [2010] for the Period 1979–2012 Against IBTrACS\_nhcjtwc

	JRA-25	JRA-55	ERA-40	ERA-Interim	CFSR	MERRA
$S_1$	0.94	0.97	0.41	0.90	0.97	0.79
RMSE	22.1	19.2	45.4	27.6	14.4	27.8
$r_{sp}$	0.94	0.95	0.85	0.90	0.96	0.94

**Table 1e.** TC Detection Verification Using *Murakami and Sugi* [2010] for the Period 1979–2012 Against IBTrACS\_nhcjtwc (90°S–90°N, All TCs)<sup>a</sup>

	JRA-25	JRA-55	ERA-40	ERA-Interim	CFSR	MERRA
Hitting rate (%)	56.8	63.2	31.2	49.7	61.7	40.3
False alarm rate (%)	24.7	25.2	35.8	28.9	29.7	33.1

<sup>a</sup>This includes hitting rate of reanalysis TCs as a reference of IBTrACS\_nhcjtwc for the period 1979–2012 and false alarm rate, which indicates the ratio of TC numbers that were detected in reanalysis but not reported in IBTrACS\_nhcjtwc. Targeted are global TCs with all TC intensity categories.

underestimate the observed TC number for most of the reanalyses, except for CFSR, indicating that TC intensity in the reanalysis is too weak for its resolution. The closest TC number was CFSR (86.0), followed by ERA-40 (47.6) and JRA-55 (39.6). On the other hand, TCs detected using *Strachan et al.* [2013] show that JRA-25 and CFSR reveal comparable TC numbers when compared to observations, whereas JRA-55 (other reanalyses) significantly overestimates (underestimate) observed TC numbers.

### 3.2. TC Track Distribution and Detection Rate

Figure 1 shows TC tracks by observations (1979–2012) and reanalysis data sets detected using *Murakami and Sugi* [2010], whereas supporting information Figure S1 shows those detected using *Strachan et al.* [2013]. Because the horizontal resolution of reanalysis output is still not sufficient to resolve observed TC inner structure, all reanalysis data sets underestimate observed TC intensity. JRA-55 and CFSR are the only data sets that have intense TCs of category 1 or stronger on the Saffir-Simpson scale. Most of the reanalyses show reasonable TC distribution globally compared with observations. Table 1d shows skill scores in terms of climatological TC frequency of occurrence, which is defined as the total count of TC positions for each analyzed grid cell (i.e., 5° × 5°) in a 6 h interval for all TCs during their lifetime. Annual mean TC frequency of occurrence was verified in terms of the Taylor Skill Score I ( $S_I$ ) [Taylor, 2001] and root-mean-square error (RMSE) as the reference for IBTrACS\_nhcjtwc. The combined influence of the spatial variance and spatial correlation,  $S_I$ , ranges from 0.0 (no skill) to 1.0 (perfect skill level). The reanalyses with the best scores are CFSR and JRA-55, followed by JRA-25 and ERA-Interim. ERA-40 showed poor skill scores because the horizontal resolution of the data set is too low, the mean length of the TC tracks is too short, and the detected TC tracks are not smoothed (see Figure 1e).

The seasonal cycle of TC frequency of occurrence is also evaluated. The bottom line of Table 1d ( $r_{sp}$ ) shows the 12 month mean spatial correlation between reanalysis and observations in terms of the climatological monthly mean TC frequency of occurrence. The correlation is high for every reanalysis, indicating that all of the reanalyses reasonably reproduce the observed seasonal variation of TC frequency of occurrence. The reanalysis with the highest correlation is CFSR, followed by JRA-55, JRA-25, and MERRA.

It is expected that TCs are detected by a reanalysis on the same date as observed. Table 1e shows results of TC detection verification. The hitting rate is computed if the observed TCs are also detected on the same date by the reanalysis and around the vicinity of the TC center within 500 km from the observed TC center. The results show that the reanalysis with the highest hitting rate was JRA-55, followed by CFSR and JRA-25. This indicates that the Japanese reanalyses and CFSR reasonably reproduce the observed TC occurrence.

In addition to the hitting rate, the false alarm rate is also evaluated. The false alarm rate is computed for all TCs detected in reanalysis. If a detected TC by reanalysis is not reported in the observation, we count it as a false alarm case. The results are shown at the bottom of Table 1e. The reanalysis with the lowest false alarm rate was JRA-25, followed by JRA-55 and ERA-Interim. Again, this indicates that the Japanese reanalyses reasonably observed TC occurrence. Most of the reanalyses show higher false alarm rates in the NIO (~60%), ENP (~30%), SIO (~35%), and SPO (~40%) than in the WNP (~18%) and NAT (~24%) (data not shown).

**Table 1f.** TC Detection Verification Using *Murakami and Sugi* [2010] for the Period 1979–2012 Against IBTrACS\_nhcjtwc (30°S–35°N,  $w_{max} \geq 64$  kt)

	JRA-25	JRA-55	ERA-40	ERA-Interim	CFSR	MERRA
Hitting rate (%)	78.1	81.1	41.2	64.3	80.4	52.0

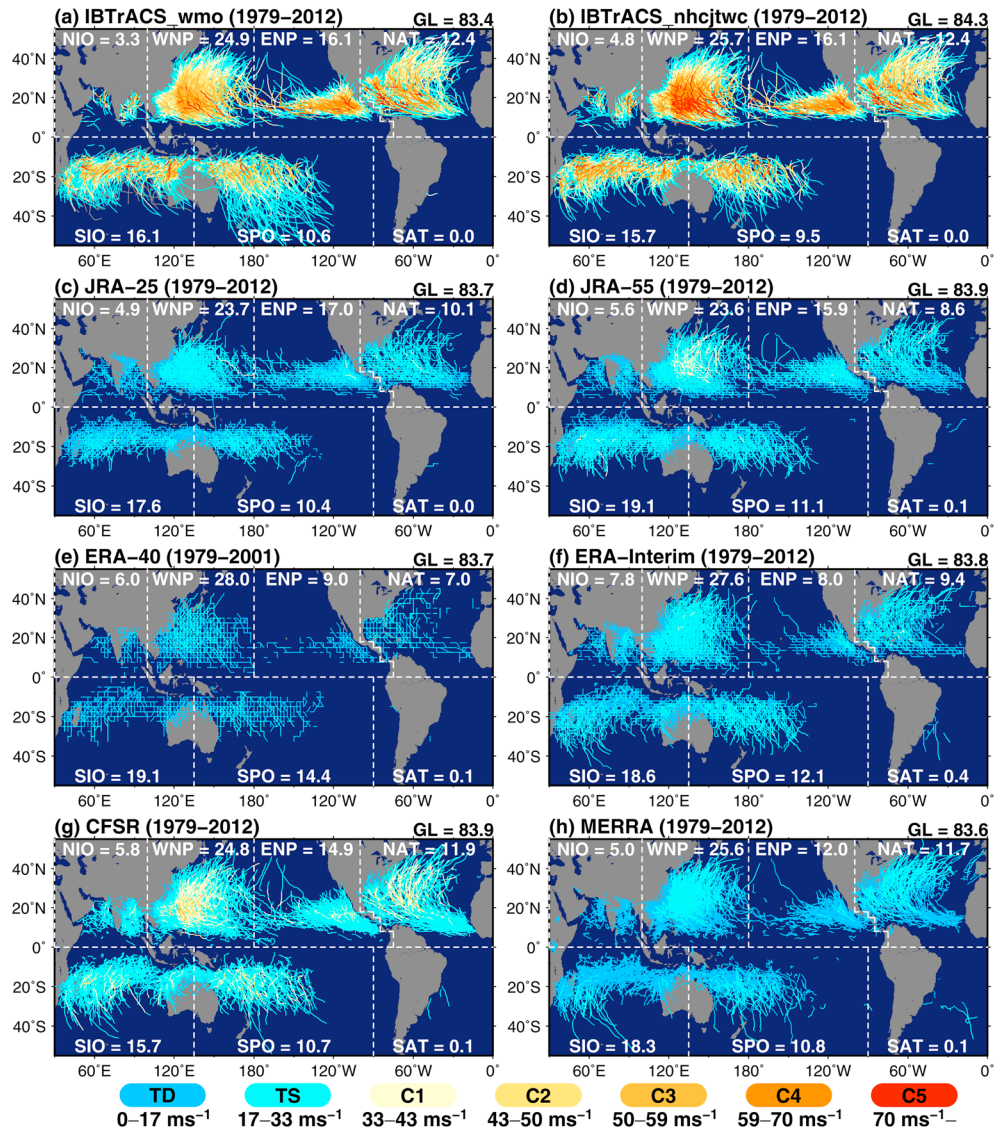


**Figure 1.** Global distribution of tropical cyclone (TC) tracks during all seasons from 1979 to 2012. Observations by (a) IBTrACS\_wmo; (b) IBTrACS\_nhcjtwc; reanalysis data sets by (c) JRA-25; (d) JRA-55; (e) ERA-40 (up to 2001); (f) ERA-Interim; (g) CFSR; and (h) MERRA. The numbers for each basin show the annual mean number of TCs. TC tracks are color coded according to the intensities of TCs as categorized by the Saffir-Simpson Hurricane Wind Scale (e.g., tropical depression (TD), tropical storms (TS), and the categories 1–5 (C1–C5)).

Because the TC tracks between IBTrACS\_wmo and IBTrACS\_nhcjtwc are inconsistent in midlatitudes, especially in the Southern Hemisphere (see Figures 1a and 1b), we only evaluate the hitting rate between 30°S and 35°N. Intense TCs may be independent of TC tracking schemes; therefore, we only evaluate observed TCs of 64 kt or stronger for the hitting rate computation. Table 1f reveals that the reanalyses with higher hitting rates are JRA-25, JRA-55, and CFSR, which is consistent with Table 1e.

### 3.3. TC Intensity

As shown in Figure 1, the reanalysis data sets systematically underestimate observed TC intensity. This may be justified because the horizontal resolution of reanalysis data sets is still too low to resolve observed TC intensity. However, the detected TC intensity must be appropriate for its resolution even though it is weaker than observed. Figure 2 shows the relationship between maximum surface wind speed (MSWS) and minimum sea level pressure (MSLP) plotted for every 6 h for detected TCs. The red dashed lines are regression curves based on observations reported by *Atkinson and Holiday [1977]*. The figure shows that the observed

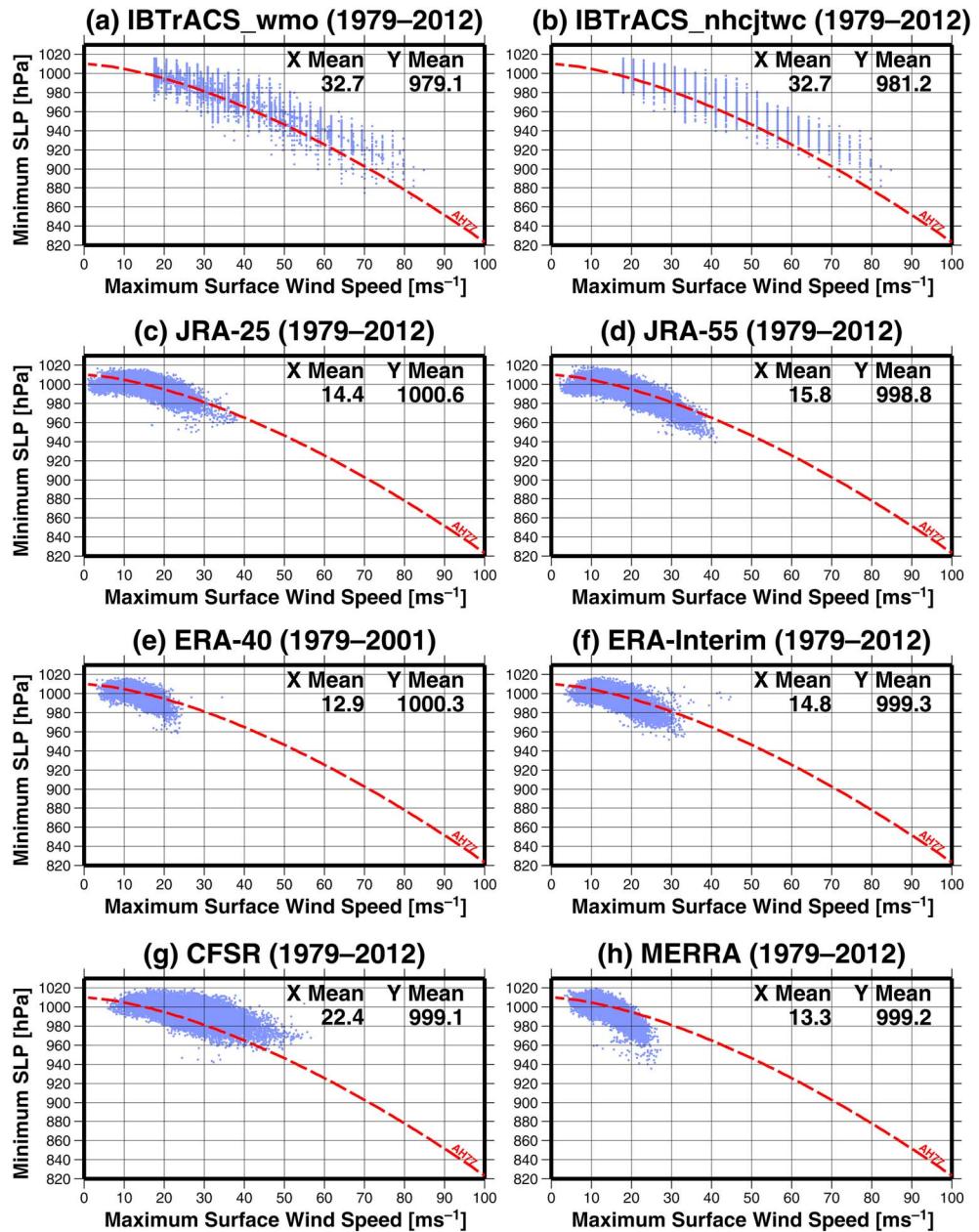


**Figure 2.** Maximum surface wind speed ( $\text{m s}^{-1}$ ) versus minimum sea level pressure (hPa) for TC: (a) IBTrACS\_wmo; (b) IBTrACS\_nhcjtwc; (c) JRA-25; (d) JRA-55; (e) ERA-40; (f) ERA-Interim; (g) CFSR; and (h) MERRA. The red curve is the regression line proposed by *Atkinson and Holiday* [1977] based on observed data. The numbers shown for each panel are the mean maximum surface wind speed (X Mean) and the minimum sea level pressure (Y Mean).

MSWS-MSLP relationship is more or less reproduced by all reanalyses especially in JRA-25, JRA-55, ERA-40, and ERA-Interim. CFSR may have larger MSWS in spite of higher MSLP, while MERRA may have lower MSLP in spite of smaller MSWS.

**3.4. Interannual Variation**

It is expected that interannual variation of detected TCs by reanalysis data sets show high correlation with observations. Supporting information Figure S2 shows the interannual variation of the annual TC number as observed and by reanalyses using *Murakami and Sugi* [2010]. The correlation coefficients between reanalyses and observations are listed in Table 2. The highest correlation coefficients for most of the ocean basins are shown by JRA-25. JRA-55 also shows significant correlations for most of the ocean basins. The highest

**Table 2.** Correlation Coefficients Between the Observed and Detected Interannual Variability of TC Genesis Number for Each Basin<sup>a</sup>

	JRA-25	JRA-55	ERA-40	ERA-Interim	CFSR	MERRA
<i>1979–2012 using Murakami and Sugi [2010]</i>						
NIO	0.08	0.25	-0.08	-0.09	0.31	<b>0.34</b>
WNP	<b>0.67</b>	<b>0.73</b>	<b>0.72</b>	<b>0.67</b>	<b>0.77</b>	<b>0.74</b>
ENP	<b>0.91</b>	<b>0.68</b>	0.28	0.14	<b>0.59</b>	<b>0.48</b>
NAT	<b>0.86</b>	<b>0.66</b>	<b>0.69</b>	<b>0.86</b>	<b>0.53</b>	<b>0.85</b>
SIO	<b>0.36</b>	<b>0.49</b>	0.22	0.30	0.23	0.25
SPO	<b>0.67</b>	<b>0.66</b>	0.41	<b>0.42</b>	<b>0.67</b>	<b>0.48</b>
<i>1958–2012 using Murakami and Sugi [2010]</i>						
NIO						
WNP		<b>0.76</b>	<b>0.57</b>			
ENP		<b>0.45</b>	0.15			
NAT		<b>0.50</b>	<b>0.57</b>			
SIO						
SPO						

<sup>a</sup>The applied TC detection method for the reanalyses is *Murakami and Sugi [2010]*. Bold numbers indicate that the correlation coefficient is statistically significant at the 95% level (Pearson's product-moment correlation significance test). IBTrACS\_nhcjtwc is used as a reference.

correlation in the WNP is shown by CFSR; however, correlations for the rest of the basins, except for SPO, are lower than those of JRA-25 and JRA-55. Most of the reanalyses show higher and significant correlations in the WNP and NAT and lower correlations in the NIO and SIO. Both CFSR and MERRA have the highest horizontal resolution among the reanalysis data sets; however, the correlation coefficients are comparable (or lower) when compared with JRA-25 and JRA-55. This indicates that horizontal resolution is not the only factor that determines higher skill in interannual variation. Our results are fairly consistent if the same analysis is applied using the TC detection method of *Strachan et al. [2013]* (see supporting information Figure S3 and Table S1).

#### 4. Summary

In this study, various state-of-the-art reanalyses of tropical cyclones (TCs) were evaluated. We used six reanalysis data sets that were released after 2004: JRA-25, JRA-55, ERA-40, ERA-Interim, CFSR, and MERRA.

The annual mean count of TCs is underestimated for most of the reanalysis data sets, except for CFSR, when the detection method of *Walsh et al. [2007]* is used. This indicates that the mean TC intensity in the reanalyses is too weak for its resolution. TCs detected using *Strachan et al. [2013]* show that JRA-25 and CFSR reveal comparable TC numbers with observations, whereas JRA-55 (other reanalyses) overestimates (underestimate) observed TC numbers. Most of the reanalyses show reasonable TC global distribution and seasonal variation compared with observations. However, all reanalyses underestimate the observed TC intensity. JRA-55 and CFSR are the only data sets that include TCs of category 1 or stronger on the Saffir-Simpson category. JRA-55 and CFSR show the highest scores in terms of climatological TC frequency of occurrence, hitting rate, and lower false alarm rate.

The relationship between maximum surface wind speed (MSWS) and minimum sea level pressure (MSLP) is evaluated to see if the reanalysis shows reasonable TC structure for its resolution. We show that the observed MSWS-MSLP relationship is adequately reproduced by all reanalysis data especially in JRA-25, JRA-55, ERA-40, and ERA-Interim. However, CFSR may have larger MSWS despite higher MSLP, while MERRA may have lower MSLP despite smaller MSWS.

The interannual variation of detected TCs by reanalyses is also evaluated. Most of the reanalyses show higher and significant correlations in the WNP and NAT and lower correlations in the NIO and SIO. JRA-25 shows the highest correlation coefficient in most of the ocean basins. JRA-55 also shows significant correlations for most of the basins. Even if the long-term data set from period 1958–2012 is used, the correlation coefficients between observations and JRA-55 were statistically significant in the WNP (0.76), ENP (0.45), and NAT (0.50). These results are mostly consistent even when using a different TC detection method, such as the one proposed by *Strachan et al. [2013]*.

Overall, we conclude that the JRA-55 appears to be the best reanalysis in terms of spatial distribution of TCs, highest hitting rate, and lower false alarm rate in the real-time observed TC frequency of occurrence, reasonable TC structure, and representation of interannual variation in TC frequency. These results suggest that the finest resolution reanalysis data sets, like MERRA, are not always the best in terms of TC climatology. The reason the Japanese reanalyses are superior to the others is that they use wind retrievals surrounding the tropical cyclone data (TCR) [Fiorino, 2002] in their assimilation systems [Hatsushika et al., 2006; Ebita et al., 2011]. TCR data are the artificial 3-D wind profile data in the vicinity of observed TCs that are created by a retrieval scheme based on Fiorino [2002] in which best-track information is used. Once the wind profile is created, the TCR data are treated as if they are observed data and are used as input data for the data assimilation process together with other observations. Hatsushika et al. [2006] compared JRA-25 with other reanalyses and a control experiment without TCR data and found that the detection rate of observed TCs in JRA-25 is higher than the others, especially in the ENP where observations are scarce.

Although it is beyond the scope of this study, the effect of the evolution of available observations and quality on TC statistics should be addressed when the long-term data sets of 1958–2012 are compared. Manning and Hart [2007] revealed a strong artificial trend in the structure of TCs in the NAT in ERA-40 due to introduction of satellite data in the data assimilation system during the 1970s. To minimize this trend, JMA is now conducting a new type of reanalysis called “JRA-55C” in which only the long-term in situ observations such as radiosonde, surface synoptic observations, and ships are included in the assimilation system.

#### Acknowledgments

H.M. would like to thank all the numerical weather prediction centers that opened their reanalysis data sets. H.M. especially thanks the Japan Meteorological Agency for providing the proto type JRA-55 data set. H.M. also thanks Pang-Chi Hsu for downloading the MERRA data and May Izumi for her editorial service. This is School of Ocean and Earth Science and Technology publication 9090 and International Pacific Research Center publication 1047.

The Editor thanks two anonymous reviewers for their assistance in evaluating this paper.

#### References

- Atkinson, G. D., and C. R. Holiday (1977), Tropical cyclone minimum sea level pressure/maximum sustained wind relationship for the western North Pacific, *Mon. Weather Rev.*, *105*, 421–427, doi:10.1175/1520-0493(1977)105<0421:TCMSLP>2.0.CO;2.
- Bell, R., J. Strachan, P. L. Vidale, K. Hodges, and M. Roberts (2013), Response of tropical cyclones to idealized climate change experiments in a global high-resolution coupled general circulation model, *J. Clim.*, *26*, 7966–7980, doi:10.1175/JCLI-D-12-00749.1.
- Dee, D. P., et al. (2011), The ERA-Interim re-analysis: Configuration and performance of the data assimilation system, *Q. J. R. Meteorol. Soc.*, *137*, 553–597, doi:10.1002/qj.828.
- Ebita, A., et al. (2011), The Japanese 55-year Reanalysis “JRA-55”: An interim report, *SOLA*, *7*, 149–152, doi:10.2151/sola.2011-038.
- Fiorino, M. (2002), Analysis and forecasts of tropical cyclones in the ECMWF 40-year reanalysis (ERA-40), *Extended Abstract of 25th Conference on Hurricanes and Tropical Meteorology*, 261–264.
- Hatsushika, H., J. Tsutsui, M. Fiorino, and K. Onogi (2006), Impact of wind profile retrievals on the analysis of tropical cyclones in the JRA-25 reanalysis, *J. Meteorol. Soc. Jpn.*, *84*, 891–905, doi:10.2151/jmsj.84.891.
- Kalnay, E., et al. (1996), The NCEP/NCAR 40-year reanalysis project, *Bull. Am. Meteorol. Soc.*, *77*, 437–471, doi:10.1175/1520-0477(1996)077<0437:TNYRP>2.0.CO;2.
- Kanamitsu, M., W. Ebisuzaki, J. Woollen, S.-K. Yang, J. J. Hnilo, M. Fiorino, and G. L. Potter (2002), NCEP-DOE AMIP-II Reanalysis (R-2), *Bull. Am. Meteorol. Soc.*, *83*, 1631–1643, doi:10.1175/BAMS-83-11-1631.
- Kawase, H., T. Yoshikane, M. Hara, F. Kimura, T. Yasunari, B. Ailikun, H. Ueda, and T. Inoue (2009), Intermodel variability of future changes in the Baiu rainband estimated by the pseudo global warming downscaling method, *J. Geophys. Res.*, *114*, D21110, doi:10.1029/2009JD011803.
- Kimura, F., and A. Kitoh (2007), Downscaling by pseudo global warming method, The Final Report of the IPCC, RIHN Project 1–1, 43–46.
- Kistler, R., et al. (2001), The NCEP-NCAR 50-year reanalysis: Monthly means CD-ROM and documentation, *Bull. Am. Meteorol. Soc.*, *82*, 247–267, doi:10.1175/1520-0477(2001)082<0247:TNNYRM>2.3.CO;2.
- Knapp, K. R., M. C. Kruk, D. H. Levinson, H. J. Diamond, and C. J. Neumann (2010), The International Best Track Archive for Climate Stewardship (IBTrACS): Unifying tropical cyclone best track data, *Bull. Am. Meteorol. Soc.*, *91*, 363–376, doi:10.1175/2009BAMS2755.1.
- Knutson, T. R., J. J. Sirutis, S. T. Garner, G. A. Vecchi, and I. M. Held (2008), Simulated reduction in Atlantic hurricane frequency under twenty-first-century warming condition, *Nat. Geosci.*, *1*, 359–364, doi:10.1038/ngeo202.
- Lauer, A., C. Zhang, O. E. Timm, Y. Wang, and K. Hamilton (2013), Downscaling of climate change in the Hawaii region using CMIP5 results: On the choice of the forcing fields, *J. Clim.*, *26*, 10,006–10,030, doi:10.1175/JCLI-D-13-00126.1.
- Manning, D. M., and R. E. Hart (2007) Evolution of North Atlantic ERA40 tropical cyclone representation, *Geophys. Res. Lett.*, *34*, L05705, doi:10.1029/2006GL028266.
- Murakami, H., and M. Sugi (2010), Effect of model resolution on tropical cyclone climate projections, *SOLA*, *6*, 73–76, doi:10.2151/sola.2010-019.
- Onogi, K., et al. (2007), The JRA-25 reanalysis, *J. Meteorol. Soc. Jpn.*, *85*, 369–432, doi:10.2151/jmsj.85.369.
- Rathmann, N. M., S. Yang, and E. Kaas (2014), Tropical cyclones in enhanced resolution CMIP5 experiments, *Clim. Dyn.*, *42*(3–4), 665–681, doi:10.1007/s00382-013-1818-5.
- Rienecker, M. M., et al. (2011), MERRA: NASA's modern-era retrospective analysis for research and applications, *J. Clim.*, *24*, 3624–2648, doi:10.1175/JCLI-D-11-00015.1.
- Saha, S., et al. (2010), The NCEP climate forecast system reanalysis, *Bull. Am. Meteorol. Soc.*, *91*, 1015–1057, doi:10.1175/2010BAMS3001.1.
- Scoccimarro, E., S. Gualdi, and A. Navarra (2012), Tropical cyclone effects on Arctic sea ice variability, *Geophys. Res. Lett.*, *39*, L17704, doi:10.1029/2012GL052987.
- Simiu, E., and R. H. Scanlon (1978), *Wind Effects on Structures*, 458 pp., Wiley InterScience, New York.
- Strachan, J., P. L. Vidale, K. Hodges, M. Roberts, and M.-E. Demory (2013), Investigating global tropical cyclone activity with a hierarchy of AGCMs: The role of model resolution, *J. Clim.*, *26*, 133–152, doi:10.1175/JCLI-D-12-00012.1.

- Taylor, K. E. (2001), Summarizing multiple aspects of model performance in a single diagram, *J. Geophys. Res. Lett.*, *106*(D7), 7183–7192, doi:10.1029/2000JD900719.
- Uppala, S. M., et al. (2005), The ERA-40 re-analysis, *Q. J. R. Meteorol. Soc.*, *131*, 2961–3012, doi:10.1256/qj.04.176.
- Waldron, K. M., J. Peagle, and J. D. Horel (1996), Sensitivity of a spectrally filtered and nudged limited-area model to outer model options, *Mon. Weather Rev.*, *124*, 529–547, doi:10.1175/1520-0493(1996)124<0529:SOASFA>2.0.CO;2.
- Walsh, K. J. E., K.-C. Ngyen, and J. L. McGregor (2004), Fine-resolution regional climate model simulations of the impact of climate change on tropical cyclones near Australia, *Clim. Dyn.*, *22*, 47–56, doi:10.1007/s00382-003-0362-0.
- Walsh, K. J. E., M. Fiorino, C. W. Landsea, and K. L. McInnes (2007), Objectively determined resolution-dependent threshold criteria for the detection of tropical cyclones in climate models and reanalysis, *J. Clim.*, *20*, 2307–2314, doi:10.1175/JCLI4074.1.